Journal of Applied Sciences

ISSN 1812-5654

science alert

ANSInet
an open access publisher
http://ansinet.com

Journal of Applied Sciences 14 (4): 325-332, 2014
ISSN 1812-5654 / DOI: 10.3923/jas.2014.325.332

Simulation and Optimization of Temperature Characteristic of Capacitive Micromachined Accelerometer System

Zhang Xia
Department of Electronic Engineering,
Xi'an University of Posts and Telecommunications, Xi'an, 710121, People's Republic of China

Abstract: The temperature characteristics of main physical parameters of a fence structure capacitive micromachined accelerometer are investigated by theoretical analysis and experiment. The experimental results show that the two initial sensing capacitances change with temperature and their variations are different from each other. Based on the temperature characteristics of the accelerometer and its interface circuit, the system-level simulation model is built on Simulink platform. The simulation results demonstrate that the mismatch between the different variations of the two initial sensing capacitances as temperature changing is the major influencing factor to the temperature performance of the accelerometer system. The greater the mismatch degree is, the more serious the temperature effect on the system becomes. The temperature performance of the accelerometer system is improved from -6.245 to -2.1 mg $°C^{-1}$ by adopting thermal resistance as the gain resistance of the instrumentation amplifier, without any additional hardware circuit or software algorithm.

Key words: Micro electromechanical system, capacitive micromachined accelerometer, temperature characteristic, simulation model

INTRODUCTION

Over the past years, MEMS (micro electromechanical system) accelerometers have developed rapidly and captured the all-important markets consisting of the consumer electronics, mobile devices, automation, industry, medical, seismometry and inertial navigation (Perlmutter and Robin, 2012; Je *et al*., 2010). Compared to other types of MEMS accelerometers, CMA (capacitive micromachined accelerometers) have several attractive advantages, such as low fabrication cost, low power dissipation, low noise, high sensitivity, high reliability, low drift and low temperature coefficient (Tan *et al*., 2011a; Sun *et al*., 2011; Chan *et al*., 2012). Therefore, many research institutes focus on the design and optimization of CMA.

The main factors which have great effects on the micromachined accelerometer system include not only the structure and mechanical parameters of the accelerometer, the noise performance of the interface circuits but also the external environment. Among many environmental factors, ambient temperature is the most important one which influences the performance of the accelerometer system significantly, such as bias stability. At present, there are many research institutes dedicating to the temperature characteristic research of micromachined accelerometer system. One of the main approaches is to keep the temperature of the accelerometer system invariable by temperature control scheme (Lakdawala and Fedder, 2004). The method will induce higher cost, larger size and more complexity. The other approach is to establish the mathematical expression between the output signal of the micromachined accelerometer system and the temperature by formula fitting or model estimation. Based on the mathematical expression, real-time temperature compensation can be accomplished by using hardware circuit or software algorithm (Weng *et al*., 2009; Yu *et al*., 2011; Zhang and Chang, 2011). In addition, several research groups analyzed the effect of the material, structure, micromachined technology, packaging on the thermal performance of micromachined accelerometer and put forward some effective optimization methods in structure design and manufacturing technology (Painter and Shkel, 2001, 2003; Chae *et al*., 2005; Yen *et al*., 2011; Tan *et al*., 2011b; Myers *et al*., 2012).

With the aim of decreasing the temperature coefficient of fence structure CMA system, a system-level simulation model with temperature built based on theoretical analysis and experiment is presented in this study. Through the simulation model, the main factor which has great effect on the temperature performance of the accelerometer system can be found and an optimizing approach will be put forward.

MATERIALS AND METHODS

Fence structure CMA: The fence structure CMA is composed of a proof-mass suspended by four U-shape springs and fence structure differential capacitors used as the sensing elements. A structure diagram of the CMA is shown in Fig. 1a and the fence structure capacitors can be simplified as shown in Fig. 1b (Zheng *et al*., 2009). The accelerometer is fabricated by bulk silicon micromachining technology. When an acceleration is applied along x-axis, the movable proof-mass will have a displacement which is transferred into the capacitance variance ΔC by changing the overlapped areas of the differential sensing capacitors, with one sensing capacitor C_{01} increasing and the other C_{02} decreasing. The sensing scheme not only achieves low damping but also eliminates the nonlinear effect.

The dynamic equation of the accelerometer is given by Eq. 1:

$$M\ddot{x}(t)+c\dot{x}(t)+k_x x(t)=Ma \quad (1)$$

where, x is the displacement of the proof-mass from its rest position with respect to the fixed frame, M is the mass of the proof-mass, k_x denotes the mechanical spring constant along x-axis and c denotes the damping factor. The input acceleration a can be obtained by measuring ΔC through the interface circuits.

Mechanical spring constant: The U-shape spring used in the fence structure CMA is helpful for residual stress releasing due to the arc part of the beam as illustrated in Fig. 2.

The mechanical spring constant of U-shape spring along x-axis can be expressed by Eq. 2 (Chen, 2004):

$$k_x=\frac{6n_sEI_z(2l+\pi r)}{2l^4+4\pi rl^3+24r^2l^2+6\pi r^3l+3\pi^2r^4-24r^4} \quad (2)$$

where $I_z = w^3t/12$ denotes inertia moment of the spring beam in z-axis, E is the Young's modulus of single-crystal silicon for <100> direction, l is the length of the straight beam, r is the inside radius of the semicircle, w and t represents the width and thickness of the spring beam separately and n_s is the total beam number.

The representative dimensions of U-shape spring are l = 1050 μm, w = 14 μm, t = 297 μm and r = 22 μm. Meanwhile, n_s and E equals to 4 and 130 GPa, respectively. With those values, k_x equals to 166.28 N m^{-1}

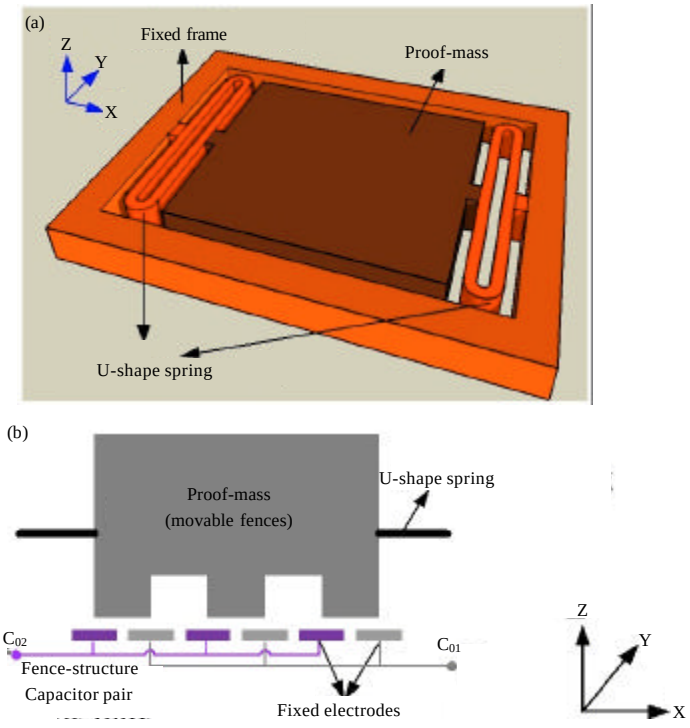

Fig. 1(a-b): (a) Structure diagram of CMA (capacitive micromachined accelerometer) and (b) Sketch map of the fence structure differential capacitors

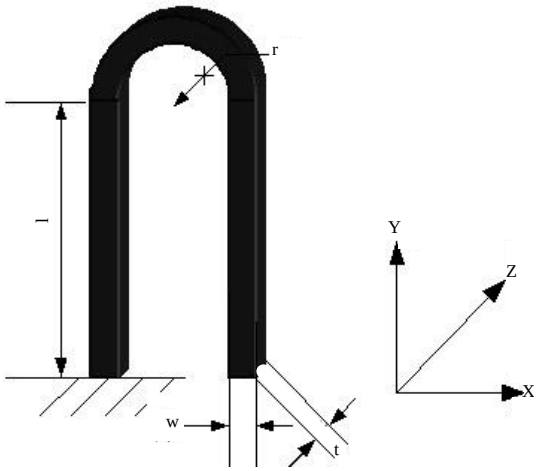

Fig. 2: Sketch map of U-shape spring

at 25°C calculated using Eq. 2. Moreover, the temperature coefficient of k_x equals to -72.5 ppm °C^{-1} by considering that the temperature coefficient of E is -75.0 ppm °C^{-1} and the Thermal Expansion Coefficient (TEC) for Si is 2.5 ppm °C^{-1}.

Damping factor: The movement of the proof-mass is in X-Y plane and the fixed electrodes are in parallel with the proof- mass, so the slide-film damping dominates in the accelerometer (Zheng, 2009). According to Couette flow model which is effective at low frequency, the slide-film damping factor is given by Bao (2000):

$$c = \frac{\mu_{eff} A}{h_0} \tag{3}$$

where, A is the surface area of the plate suffering damping force, h_0 is the gap distance between the proof-mass and the fixed electrodes, μ_{eff} represents the effective viscosity coefficient and can be described by Veijola and Turowski (2001):

$$\mu_{eff} = \frac{\mu}{1 + 2 \cdot K_n + 0.2 \cdot K_n^{0.788} \cdot e^{-K_n/10}} \tag{4}$$

where, K_n is the Knudsen number, it is the ratio between the mean free path of the molecules λ and gap distance h_0: $K_n = \lambda/h_0$, $\mu = \rho\bar{v}\lambda/3$ represents the viscosity coefficient, $\bar{v}$ denotes the average velocity of the gas molecules and $\bar{v} = \sqrt{8RT/(\pi M_{ol})}$, the gas density $\rho = PM_{ol}/RT$ according to Clapeyron equation, R is gas constant, M_{ol} is the molar mass of the gas, P is the gas pressure and T is temperature in Kelvin.

The expression of the mean free path is (Bird, 1983):

$$\lambda = \frac{1}{\sqrt{2}\pi d_0^2 n} \tag{5}$$

where, πd_0^2 represents the molecular collision cross-sectional area, n is the number density of molecules which can be expressed by $n = P/k_BT$ for ideal gas, k_B is Boltzmann constant.

Thus, with Eq. 3-5, the expression of *c* can be drawn out:

$$c = \frac{2}{3} \cdot \sqrt{\frac{M_{ol} \cdot (t + 273)}{\pi^3 R}} \cdot \frac{k_B}{d_0^2 \cdot K_n'} \cdot \frac{L \cdot W}{h_0} \tag{6}$$

With:

$$K_n' = 1 + 2 \cdot (\lambda/h_0) + 0.2 \cdot (\lambda/h_0)^{0.788} \cdot e^{-(\lambda/h_0)/10}$$

Where:
L: The length of the proof-mass
W: The width of the proof-mass
t: Temperature in °C

In addition, $k_B = 1.38\times10^{-23}$ J K^{-1}, $d_0 = 3.74\times10^{-10}$ m, R = 8.314 Pa•m^3 mol^{-1}•K, $M_{ol} = 29\times10^{-3}$ kg mol^{-1} and $P = 1.013\times10^5$ Pa due to the unsealed package of the accelerometer. The typical dimensions of the fence structure CMA are $h_0 = 1.7$ μm, L×W = 2200 μm×2360 μm, the thickness of the proof-mass is 297.7 μm, the thickness of Al electrode is 0.6 μm and the thickness of fixed frame is 300 μm. All dimensions are affected by thermal expansion of materials certainly. TEC of Si is 2.5 ppm °C^{-1} and TEC of Al is 23.6 ppm °C^{-1}. Combining Eq. 6, it can be got that c equals to 3.3525×10^{-5} Nm sec^{-1} at 25°C and its temperature coefficient is 1650.4 ppm °C^{-1}.

EXPERIMENT AND SIMULATION

Experimental test: The macro expression of the spring constant can be expressed as:

$$k_x = \omega_0^2 M \tag{7}$$

where ω_0 is the resonant angular frequency of the accelerometer, $M = 3.619\times10^{-6}$ Kg represents the mass of the proof-mass.

The macro expression of the damping factor is given by:

$$c = 2\pi M \Delta f \tag{8}$$

where, Δf denotes 3 dB bandwidth.

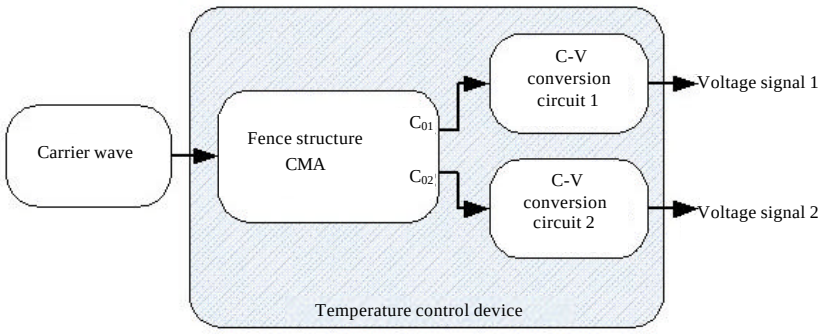

Fig. 3: Test condition for initial sensing capacitance

Table 1: Spring constant, damping factor and their temperature coefficients

Parameters	k_x at 25°C (N/m)	Temperature coefficient of k_x (ppm °C^{-1})	c at 25°C (Nm sec^{-1})	Temperature coefficient of c (ppm °C^{-1})
0#	188.44	-53.40	1.6871×10^{-4}	1202.06
1#	573.59	-57.14	1.9687×10^{-4}	805.96
2#	558.09	-59.59	1.5741×10^{-4}	1146.61

Table 2: Initial sensing capacitances and their temperature coefficients

Accelerometers	Capacitancet at 25°C (pF)	Temperature coefficient (ppm °C^{-1})	Capacitance variation with temperature (fF °C^{-1})
0#			
C_{01}	5.9413	211.76	1.26
C_{02}	6.4774	283.53	1.84
1#			
C_{01}	2.8233	309.87	0.86
C_{02}	3.6870	90.97	0.34
2#			
C_{01}	6.0303	367.86	2.22
C_{02}	6.2498	321.01	2.01

Based on Eq. 7, 8, the spring constant and the damping factor can be calculated by measuring ω_0 and Δf under different temperatures, when an external driving signal with constant amplitude and variable frequency is applied to the accelerometer. The experimental results are listed in Table 1.

From Table 1, it can be seen that the spring constants k_x of different accelerometers are not the same due to different beam widths in design while the temperature coefficients of k_x are all in the range of -60~-50 ppm °C^{-1} which is agree well with the theoretical analysis. The damping factors and their temperature coefficients show greater differences from the theoretical analysis. One of the reasons is due to the slots on the proof-mass which increases the air damping. The other is the theoretical error of slide-film damping induced by the simplified Couette flow model.

Initial sensing capacitance: The initial sensing capacitance of the fence structure CMA can be expressed as:

$$C_0 = \frac{N\varepsilon x_0 y_0}{h_0} \quad (9)$$

where, ε is dielectric constant, N is the number of fingers, y_0 and x_0 denotes the overlap length and overlap width, respectively, h_0 is the gap distance.

In order to measure the temperature coefficients of the two initial sensing capacitances, the accelerometer was put in the temperature control device and a constant carrier wave was applied to the sensor. The test condition is shown in Fig. 3. C-V (capacitance-voltage) conversion circuit can convert the capacitance of the accelerometer to an amplified voltage signal proportionally. In the experiment, the amplitudes of the two voltage signals were measured by Agilent digital multimeter when the temperature was ranging from 25 to 65°C at intervals of 5°C. Consequently, C_{01} and C_{02} and their temperature coefficients could be obtained. The experimental results are shown in Table 2.

Table 2 indicates that the two initial sensing capacitance C_{01} and C_{02} in the same accelerometer are not equal or their temperature coefficients differ from each other either. One reason for this is that the overlap width x_{01} differs from x_{02} due to the imprecise align of alignment marks and the nonideal packaging for accelerometer during manufacturing process. On the one hand, temperature influence on the initial sensing capacitances is caused by thermal expansion and contraction of materials which change the overlapped area and the gap distance. Furthermore, there is thermal stress among the layers of the accelerometer which is a function of temperature because each layer has its own thermal expansion coefficients. Thermal stress also induces the

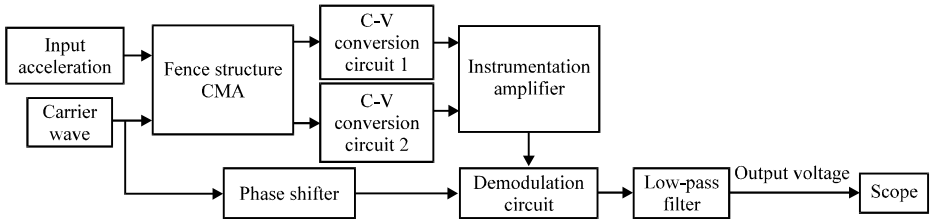

Fig. 4: System-level model for fence structure CMA system (built on Simulink)

initial sensing capacitances to change with temperature. As well as thermal stress, residual stress affects the temperature characteristic of the initial sensing capacitances directly. MEMS technology such as high temperature oxidation and high temperature bonding could induce residual stress among the layers. In addition, residual stress also exists in the spring beams due to the defects formed during fabrication, although the circular part of U-shape spring beam is good for stress release to a certain extent.

Establishment and verification of the temperature model: We have reported a system-level simulation model of fence structure CMA system based on Simulink platform (Zhang *et al*., 2010). The model could simulate noise performance. On this basis, temperature factor was taken into account. The temperature-dependent parameters in the accelerometer include spring constant, damping factor and initial sensing capacitances. Furthermore, the model contains parameters which could be affected by temperature in the interface circuits, such as amplifier input offset voltage, amplifier input offset current, gain, gain error, thermal noise, resistance, capacitance and so on. The system-level simulation model with the mechanical parameters of the accelerometer 0# and its interface circuits is shown in Fig. 4.

In order to investigate the temperature performance of the accelerometer system, the accelerometer and its interface circuits were all put in the temperature control device. The output voltage under zero acceleration was measured with temperature ranging from 25 to 65°C at intervals of 5°C. Meanwhile, the simulation was performed under the same conditions. The experimental result and the simulation result are illustrated in Fig. 5.

As shown in Fig. 5, it is clear that the simulation result is agree well with the experimental result which not only verifies the correctness of the simulation model but also best illustrates that the mechanical parameters such as spring constant, damping factor and initial sensing capacitances and all circuit parameters took into account in the model can reflect the temperature performance of the accelerometer system elaborately. Meanwhile, Fig. 5

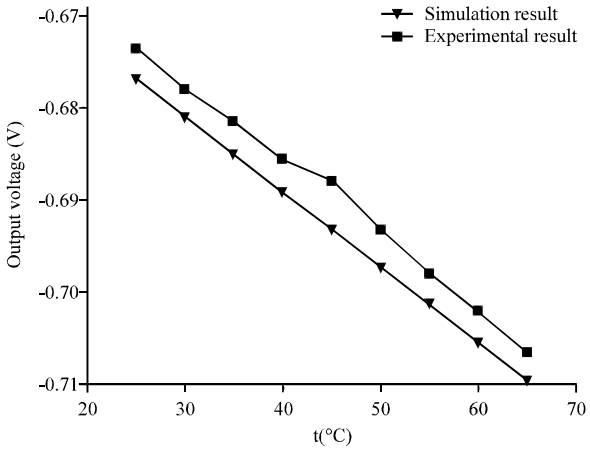

Fig. 5: Output voltage of fence structure CMA system versus temperature (including experimental results and simulation results)

shows that the absolute value of the output voltage in simulation is a little higher than the experimental result. The reason is the two input signals of the synchronous demodulation circuit are not in phase perfectly in the experiment. From the linear fitting curve of the experimental result, it can be got that the temperature coefficient of the output voltage is -0.818 mV $°C^{-1}$ which corresponds to an effective acceleration variation of -6.245 mg $°C^{-1}$ with the sensitivity 131 mV g^{-1}. The sensitivity test of the accelerometer system is performed on a circular dividing table. By collecting the output dc voltage of the system using Agilent digital multimeter every 5° and linear data fitting, the system sensitivity is obtained. The result above shows that the temperature has a significant influence on the bias stability of the fence structure CMA system.

RESULTS AND DISCUSSION

In order to decrease the temperature coefficient of the fence structure CMA system, the most important factor influencing the system temperature performance was found based on the simulation model. Table 3 illustrates

Table 3: Main factors influencing the temperature performance of the accelerometer system

Simulation parameter settings	System temperature coefficient (mg °C^{-1})	Reduction percentage of the temperature coefficient (%)
When the variations of the two initial sensing capacitances with temperature is the same	-0.640	89.74
When the temperature coefficient of the spring constant is zero	-6.243	0.03
When the temperature coefficient of the damping factor is zero	-6.243	0.03
When the temperature coefficients of the interface circuits are zero	-5.575	10.73

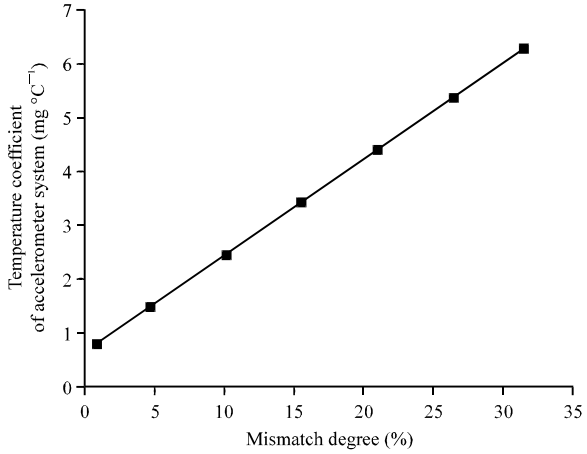

Fig. 6: Temperature coefficient of fence structure CMA system versus mismatch degree

the simulation results under different situations. It can be observed that the temperature coefficient of the accelerometer system has been reduced to -0.64 mg °C^{-1}, when the variations of the two initial sensing capacitances with temperature were set to be the same accurately in the model. Therefore, the temperature characteristic of C_{01} and C_{02} is the most major factor influencing the system temperature performance. The secondary factor is the temperature characteristic of interface circuits.

From Table 2, it can be seen that capacitance variations of C_{01} and C_{02} with temperature differ from each other. So, we use mismatch degree to calibrate the difference. The expression of the mismatch degree is shown as:

$$\text{Mismatch degree} = \frac{\left(TC_{C_{01}} - TC_{C_{02}}\right)}{TC_{C_{01}}} \times 100\% \quad (10)$$

where TC_{C01} and TC_{C02} is the capacitance variation of C_{01} and C_{02} as temperature changing respectively. The relationship between mismatch degree and system temperature coefficient is illustrated in Fig. 6 which was obtained from the simulation model.

It is evident that the higher the mismatch degree is, the stronger the temperature influence on the output voltage of the accelerometer system becomes. In order to optimize the system temperature performance, the unequal variations of C_{01} and C_{02} with temperature should be compensated. The output dc voltage of the accelerometer system at 25°C can be expressed as:

$$V_{out} = V_{carrier} \cdot \frac{(C_{01} - C_{02})}{C_f} \cdot G_{IN} \cdot G_D \cdot G_{LP} \quad (11)$$

where, $V_{carrier}$ is the amplitude of carrier wave, C_f is the feedback capacitance of C-V conversion circuit, G_{IN} is the gain of instrumentation amplifier, G_D and G_{LP} represents the gains of the demodulation circuit and the low-pass filter, respectively.

When the temperature changes Δt, the output dc voltage becomes:

$$V_{out}' = V_{carrier} \cdot (1 + K_{TC1} \cdot \Delta t) \cdot \frac{\left[C_{01} \cdot (1 + K_{TC2} \cdot \Delta t) - C_{02} \cdot (1 + K_{TC3} \cdot \Delta t)\right]}{C_f \cdot (1 + K_{TC4} \cdot \Delta t)} \cdot G_{IN} \cdot (1 + K_{TC5} \cdot \Delta t) \cdot G_D \cdot (1 + K_{TC6} \cdot \Delta t) \cdot G_{LP} \cdot (1 + K_{TC7} \cdot \Delta t) \quad (12)$$

where, K_{TC2} and K_{TC3} represent the temperature coefficients of C_{01} and C_{02}. K_{TC5} is the temperature coefficient of G_{IN}. K_{TC1}, K_{TC4}, K_{TC6} and K_{TC7} are the temperature coefficients of $V_{carrier}$, C_f, G_D, G_{LP}, respectively and they are all smaller than 20 ppm °C^{-1}. Neglecting K_{TC1}, K_{TC4}, K_{TC6} and K_{TC7}, Eq. 12 can be simplified as:

$$V_{out}' = V_{carrier} \cdot \frac{\left[C_{01} \cdot (1 + K_{TC2} \cdot \Delta t) - C_{02} \cdot (1 + K_{TC3} \cdot \Delta t)\right]}{C_f} \cdot G_{IN} \cdot (1 + K_{TC5} \cdot \Delta t) \cdot G_D \cdot G_{LP} \quad (13)$$

Equation 13 shows that choosing K_{TC5} rationally could compensate the difference between K_{TC2} and K_{TC3} and decrease the temperature coefficient of the accelerometer system. The gain of the instrumentation amplifier AD8221 is expressed as:

$$G_{IN} = 1 + \frac{49.4\,k\Omega}{R_G} \quad (14)$$

where, R_G is the gain resistance. Therefore, K_{TC5} could be changed by adjusting the temperature coefficient of R_G. In this study, we use a thermal resistor with 1600 ppm °C^{-1}

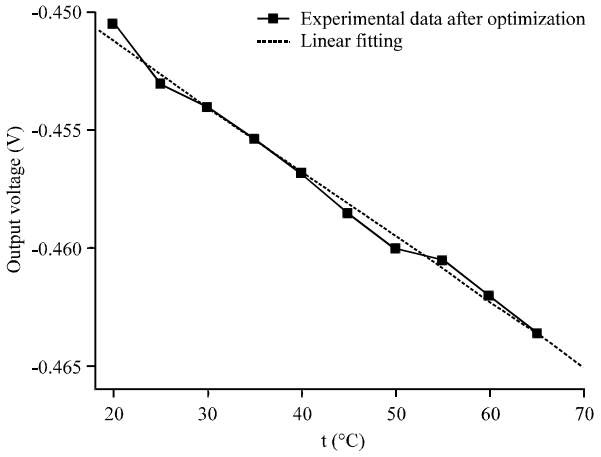

Fig. 7: Output voltage of fence structure CMA system versus temperature after optimization (experimental results)

and resistance 3.6 kΩ at 25°C as the gain resistance of the instrumentation amplifier to compensate the unequal variations of C_{01} and C_{02} with temperature. The optimized accelerometer system was measured with temperature ranging from 20 to 65°C at intervals of 5°C. The test result is shown in Fig. 7 and the slope of the linear fitting curve decreases to -0.275 mV °C^{-1} which corresponds to -2.1 mg °C^{-1}.

The experimental result after optimization shows that using thermal resistor with high temperature coefficient as the gain resistance of the instrumentation amplifier could reduce the system temperature drift drastically. What's more, the optimized system is the same as before in size and complexity, owing to no additional hardware circuit or software algorithm used for temperature compensation.

CONCLUSION

In this study, the relationship between the main physical parameters of the accelerometer and the ambient temperature was obtained through theoretical analysis and experiment. The main influencing factor of the temperature performance of the fence structure capacitive micromachined accelerometer system was found to be the mismatch between variations of the two initial sensing capacitances with temperature. The system was optimized by replacing ordinary gain resistance of the instrumentation amplifier with thermal resistance and the system temperature coefficient was reduced to -2.1 mg °C^{-1} which is 33.6% as before. In the future, a more effective optimization method will be proposed by simulation model and applied to this accelerometer system.

ACKNOWLEDGMENTS

This study was supported by research foundation project for Young Teachers of Xi'an University of Posts and Telecommunications, People's Republic of China. (101-0477).

REFERENCES

Bao, M.H., 2000. Micro Mechanical Transducers: Pressure Sensors, Accelerometers and Gyroscopes. Elsevier, Netherlands, ISBN-13: 9780080524030, pp: 123-137.

Bird, G.A., 1983. Definition of mean free path for real gases. Phys. Fluids, 26: 3222-3223.

Chae, J., H. Kulah and K. Najafi, 2005. A monolithic three-axis micro-g micromachined silicon capacitive accelerometer. J. Microelectromech. Syst., 14: 235-242.

Chan, C.K., S.C. Lo, Y.C. Huang, M. Wu, M.Y. Wang and W. Fang, 2012. Poly-Si based two-axis differential capacitive-sensing accelerometer. IEEE Sensors J., 12: 3301-3308.

Chen, Y., 2004. Research of tuning fork type micromachined gyroscope based on slide-film damping. Ph.D. Thesis, Shanghai Institute of Microsystem and Information Technology, Shanghai, China.

Je, C.H., S. Lee, M.L. Lee, J. Lee, W.S. Yang and C.A. Choi, 2010. Z-axis capacitive MEMS accelerometer with moving ground masses. Proceedings of the IEEE Sensors Conference, November 1-4, 2010, Waikola, HI., USA., pp: 635-638.

Lakdawala, H. and G.K. Fedder, 2004. Temperature stabilization of CMOS capacitive accelerometers. J. Micromechan. Microeng., Vol. 14. 10.1088/0960-1317/14/4/017

Myers, D.R., R.G. Azevedo, L. Chen, M. Mehregany and A.P. Pisano, 2012. Passive substrate temperature compensation of doubly anchored double-ended tuning forks. J. Microelectromech. Syst., 21: 1321-1328.

Painter, C.C. and A.M. Shkel, 2001. Structural and thermal analysis of a MEMS angular gyroscope. Proceedings of the 8th Annual International Symposium on Smart Structures and Materials, March 4-8, 2001, Newport Beach, CA., USA., pp: 4334-4342.

Painter, C.C. and A.M. Shkel, 2003. Structural and thermal modeling of a z-axis rate integrating gyroscope. J. Micromechan. Microeng., 13: 229-237.

Perlmutter, M. and L. Robin, 2012. High-performance, low cost inertial MEMS: A market in motion. Proceedings of the IEEE/ION Position Location and Navigation Symposium, April 23-26, 2012, Myrtle Beach, SC., USA., pp: 225-229.

Sun, H., D. Fang, K. Jia, F. Maarouf, H. Qu and H. Xie, 2011. A low-power low-noise dual-chopper amplifier for capacitive CMOS-MEMS accelerometers. IEEE Sensors J., 11: 925-933.

Tan, S.S., C.Y. Liu, L.K. Yeh, Y.H. Chiu and K.Y. Hsu, 2011a. A new process for CMOS MEMS capacitive sensors with high sensitivity and thermal stability. J. Micromechan. Microeng., Vol. 21. 10.1088/0960-1317/21/3/035005

Tan, S.S., C.Y. Liu, L.K. Yeh, Y.H. Chiu, M.S. Lu and K.Y. Hsu, 2011b. An integrated low-noise sensing circuit with efficient bias stabilization for CMOS MEMS capacitive accelerometers. IEEE Trans. Circ. Syst. I: Regul. Pap., 58: 2661-2672.

Veijola, T. and M. Turowski, 2001. Compact damping models for laterally moving microstructures with gas-rarefaction effects. J. Microelectromech. Syst., 10: 263-273.

Weng, H.N., X.M. Hu, Z. Pei, X. Cheng and J.L. Yang, 2009. Novel method of temperature error compensation for accelerometer. J. Chin. Inertial Technol., 17: 479-482.

Yen, T.H., M.H. Tsai, C.I. Chang, Y.C. Liu and S.S. Li *et al*., 2011. Improvement of CMOS-MEMS accelerometer using the symmetric layers stacking design. Proceedings of the IEEE Sensors Conference, October 28-31, 2011, Limerick, Ireland, pp: 145-148.

Yu, X.T., L. Zhang, L.R. Guo, F. Zhou and H. Yu, 2011. Temperature modeling and compensation of accelerometer based on least squares wavelet support vector machine. J. Chin. Inertial Technol., 19: 95-98.

Zhang, L. and J. Chang, 2011. A method of identification of temperature model and temperature compensation for the MEMS accelerometer. Chin. J. Sensors Actuators, 24: 1551-1555.

Zhang, X., H. Wang, X.D. Zheng, S.C. Hu and Z.H. Jin, 2010. Modeling and noise analysis of a fence structure micromachined capacitive accelerometer system. J. Zhejiang Univ. Sci. C, 11: 1009-1015.

Zheng, X.D., 2009. Study of micromachined inertial sensors based on a novel comb-bar capacitor scheme. Zhejiang University, Hangzhou, China, pp: 48-49.

Zheng, X.D., Z.H. Jin, Y.L. Wang, W.J. Lin and X.Q. Zhou, 2009. An in-plane low-noise accelerometer fabricated with an improved process flow. J. Zhejiang Univ. Sci. A, 10: 1413-1420.